ATMOSPHERIC SCIENCE

Two decades of human- and climate-induced groundwater storage shifts in Brazil

Augusto Getirana[1,2]*†, Clyvihk Renna Camacho[3,4]*†, Maria Antonieta A. Mourão[3], Otto Corrêa Rotunno Filho[4]

Brazil holds the world's largest reserves of renewable fresh water, yet recurrent water crises expose its growing vulnerability under extreme events. As the nation's groundwater demand increases, these reserves still are poorly monitored. Here, we present a data-driven spatiotemporal reconstruction of Brazil's groundwater behavior over the past two decades, integrating multi-satellite and in situ data into an artificial intelligence modeling framework. Results reveal groundwater variability, recharge, and emerging trends under climatological and anthropogenic stressors across the nation's ~8.5 million km^2 of land. Brazil's mean groundwater recharge in aquifer outcrop zones during 2002–2023 was 223 ± 16 mm year^{-1}, corresponding to ~12% of mean annual precipitation in those areas. When integrated over the analyzed outcrop extent, this corresponds to a natural recharge flux of ~1900 ± 136 km^3 year^{-1}. Persistent depletion or no recharge is observed in heavily exploited aquifers in eastern Brazil, further impacted by prolonged droughts and climate oscillations. Such aquifers present level declines mirroring patterns observed in intensively exploited aquifers in Bangladesh, India, Iran, and the US. As a world's major breadbasket, Brazil plays a vital role in global food security. Results presented here are therefore critical to the nation's sustaining agricultural productivity under increasing climate stress.

INTRODUCTION

Brazil has the world's largest volume of renewable fresh water, contributing roughly 20% of global inland runoff to the oceans (*1*). However, this abundance has not shielded the country from water insecurity. Over the past three decades, Brazil has experienced three major nationwide water crises—2000–2001, 2014–2017, and 2021—each intensified by climate-driven drought events and the nation's reliance on surface water sources. These crises underscore the urgent need to diversify water supplies and strengthen resilience through increased understanding and sustainable use of groundwater resources (*2*).

Beneath Brazil's 8.5 million km^2 of land lies a vast reserve of groundwater. Groundwater storage (GWS) is coarsely estimated in 112,000 km^3 (*3*), or ~95% of Brazilian water reserves (*4*). Over half of Brazilian municipalities draw on aquifers to some extent, and along with agricultural demand, groundwater accounts for ~55% of the nation's water demand (*5*). As a result, concerns about declining GWS have grown, with recent studies highlighting regional depletion trends (*1*, *6*–*9*). Despite this, Brazil's national groundwater monitoring infrastructure remains limited—about 500 federal wells provide sparse and uneven coverage across the country (*6*, *10*). This data scarcity hampers efforts to characterize the spatial and temporal dynamics of aquifer systems and to manage them sustainably.

Spatiotemporal large-scale groundwater monitoring in Brazil has been limited to modeling attempts based on global datasets. Earth Observing datasets, such as NASA's Gravity Recovery and Climate Experiment (GRACE) (*11*), have been used as a proxy to quantify groundwater loss (*2*, *12*). Such studies give us a first-order picture of Brazil's groundwater dynamics, but uncertainties remain high due to little to no integration of local data.

Appropriate hydrogeological monitoring at different scales faces difficulties related to geological complexity, diversity, and corresponding structures. Other factors affecting monitoring are complexities related to hydraulic properties of aquifers, recharge zones, groundwater exploitation, land use and land cover change, as well as meteorological and climate variability (*6*, *13*). Parameterizing such a large number of factors without their adequate spatial and temporal distribution is a challenge to groundwater numerical modeling (*14*).

Surrogate models, without physical coupling (*15*), such as those based on artificial intelligence (AI), can simulate the behavior of groundwater without the need for in-depth recognition of the geological environment (*14*, *16*–*18*) with results that already surpass physical models (*6*, *19*–*21*). Building upon recent developments combining GRACE data and hydrogeological measurements within an AI modeling framework (*6*), we reconstructed 21 years of spatiotemporal groundwater variability across Brazil. Our AI modeling framework ingests multi-source hydrogeological and meteorological data, including a variety of ground and satellite measurements and Brazil's hydrogeomorphology and water use information for a more precise groundwater monitoring across the country. The AI model is capable of filling the gaps between gauges, providing detailed groundwater variability across the country, never before observed. As a result, we were able to characterize Brazil's GWS dynamics, unraveling its spatially distributed emerging trends, and impacts of climatological events.

RESULTS

Groundwater variability across Brazilian aquifers

GWS SD (σ) serves as a proxy for temporal variability and provides insights into the interplay between hydrological processes and unconfined aquifer characteristics. Figure 1 shows the spatial distribution of GWS variability, including long-term maxima, minima, and seasonal patterns. High σ values are found in regions where both natural (e.g., climate, lithology, and surface-subsurface connectivity) and anthropogenic factors (e.g., groundwater abstraction and land use) drive dynamic groundwater behavior. Notably, the highest GWS

[1]Hydrological Sciences Laboratory, NASA Goddard Space Flight Center, Greenbelt, MD, USA. [2]Science Systems and Applications Inc., Lanham, MD, USA. [3]Geological Survey of Brazil, Belo Horizonte, Brazil. [4]Civil Engineering Department, Federal University of Rio de Janeiro, Rio de Janeiro, Brazil.
*Corresponding author. Email: augusto.getirana@nasa.gov (A.G.); clyvihk.camacho@sgb.gov.br (C.R.C.)
†These authors contributed equally to this work.

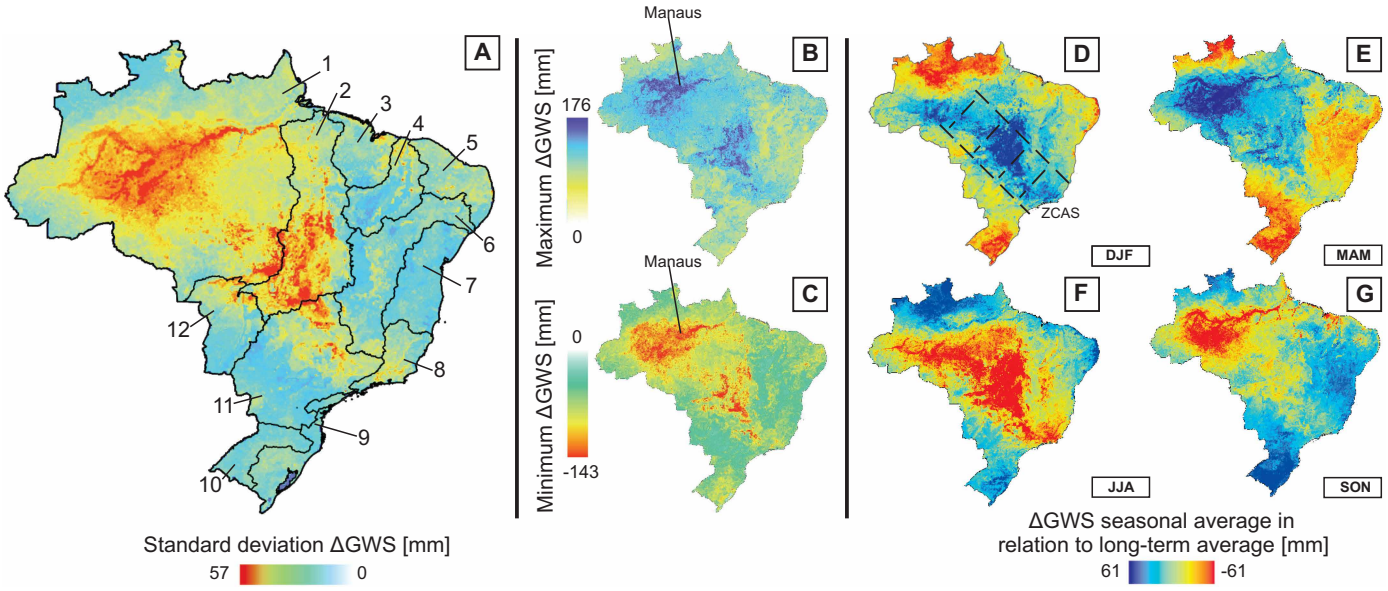

Fig. 1. Spatial and seasonal variability of simulated groundwater storage anomalies (ΔGWS) in Brazil. (A) SD of monthly ΔGWS across the 2002–2023 simulation period. (**B**) Minimum and (**C**) maximum monthly ΔGWS values. (**D** to **G**), Seasonal ΔGWS anomalies for austral summer (DJF), autumn (MAM), winter (JJA), and spring [September-October-November (SON)], computed as the deviation from the long-term seasonal mean (2002–2023). The main zone of South Atlantic Convergence (SACZ) activity is outlined on the DJF map. Twelve major hydrographic basins are delineated in (A): (1) Amazon, (2) Tocantins-Araguaia, (3) Western North-East Atlantic, (4) Parnaíba, (5) North-East Atlantic, (6) São Francisco, (7) Eastern Southeast Atlantic, (8) Southeast Atlantic, (9) South Atlantic, (10) Uruguay, (11) Paraná, and (12) Paraguay.

variability occurs in more transmissive alluvial deposits of northwestern Brazil, within the Amazon basin ($\sigma = 50$ mm), and in the fractured crystalline basement of central Brazil ($\sigma = 37$ to 43 mm), where aquifers are typically shallower due to their lithological properties and enhanced surface-groundwater connectivity (*10*, *22*, *23*) (see fig. S1 for GWS variability of outcrop zones of selected aquifers and text S1 for their brief characterization).

Within the Amazon basin, particularly at the confluence of the Solimões and Negro Rivers, near Manaus, GWS anomalies range from +176 mm to −143 mm (Fig. 1, B and C). This location is characterized by surface water level variations of 10 to 15 m (*24*), which likely exert strong influence on subsurface water storage due to intense surface-aquifer coupling (*25*). Although the basin is predominantly composed of porous sedimentary aquifers, extensive crystalline bedrock regions—less favorable for groundwater retention—are also present (*26*, *27*). These conditions, combined with the region's flat topography, high hydrological seasonality, and strong river-aquifer interactions, may contribute to recent drought episodes in the Amazon's river systems (*28*). Our model captures these dynamics, showing finer-resolution river patterns with substantially elevated GWS variability ($\sigma = 57$ mm), compared to the remainder of the basin ($\sigma = 22$ mm).

In contrast, lower GWS variability is observed across free and porous aquifers in central and northeastern Brazil, with aquifer-averaged SDs ranging from 10 to 13 mm. This reduced variability is likely associated with deeper static groundwater levels (*22*), which confer a greater capacity to buffer seasonal or interannual hydrological fluctuations compared to shallow alluvial or unconsolidated sedimentary systems that display greater ΔGWS amplitudes.

The AI-based modeling framework also reveals groundwater variability patterns linked to the South Atlantic Convergence Zone (SACZ) (*29*). SACZ plays a key role in transporting moisture from the Amazon basin toward central and southeastern Brazil, particularly during the austral summer [December-January-February (DJF)] (*30*). This influence is evident in Fig. 1D, which highlights a pronounced belt of wetter-than-average GWS conditions extending from the Amazon to southeastern Brazil during DJF months. Conversely, during June-July-August (JJA), widespread groundwater reduction occurs across central Brazil, driven by seasonal drought, baseflow discharge, and elevated evapotranspiration (ET) losses (*31*).

Groundwater recharge

Aquifer recharge, defined as the annual variation in GWS, was estimated across Brazil using the water table fluctuation (WTF) method (*32*–*35*) for each hydrological year between 2002 and 2023, focusing on unconfined aquifer systems. The calculation was performed using modeled GWS. The output is continuous over time; however, 2017 was excluded from the computation because it coincided with the data gap (~11 months) between the GRACE and GRACE-FO (Follow-On) missions. The national mean annual recharge during this period was 223 ± 16 mm year^{-1}, corresponding to a total volume of approximately 1900 ± 136 km^3 year^{-1}. This volume represents roughly 12% of the country's average annual precipitation.

Recharge rates exhibit significant spatial variability (Fig. 2A). For instance, the carbonate portion of the Bambuí karst aquifers displays relatively high recharge efficiency, capturing up to 18% of local precipitation (fig. S2). In contrast, fractured aquifers exhibit lower recharge rates, capturing approximately 5% of rainfall, while granular aquifers yield an average recharge rate of 12.5%.

Temporal variability in recharge is also pronounced. The lowest annual recharge was recorded in 2015, at 159 ± 16 mm year^{-1} (1354 ± 136 km^3 year^{-1}), coinciding with a widespread drought that triggered a national water crisis (*1*). Conversely, the highest recharge occurred in 2021, reaching 274 ± 16 mm (2333 ± 136 km^3 year^{-1}).

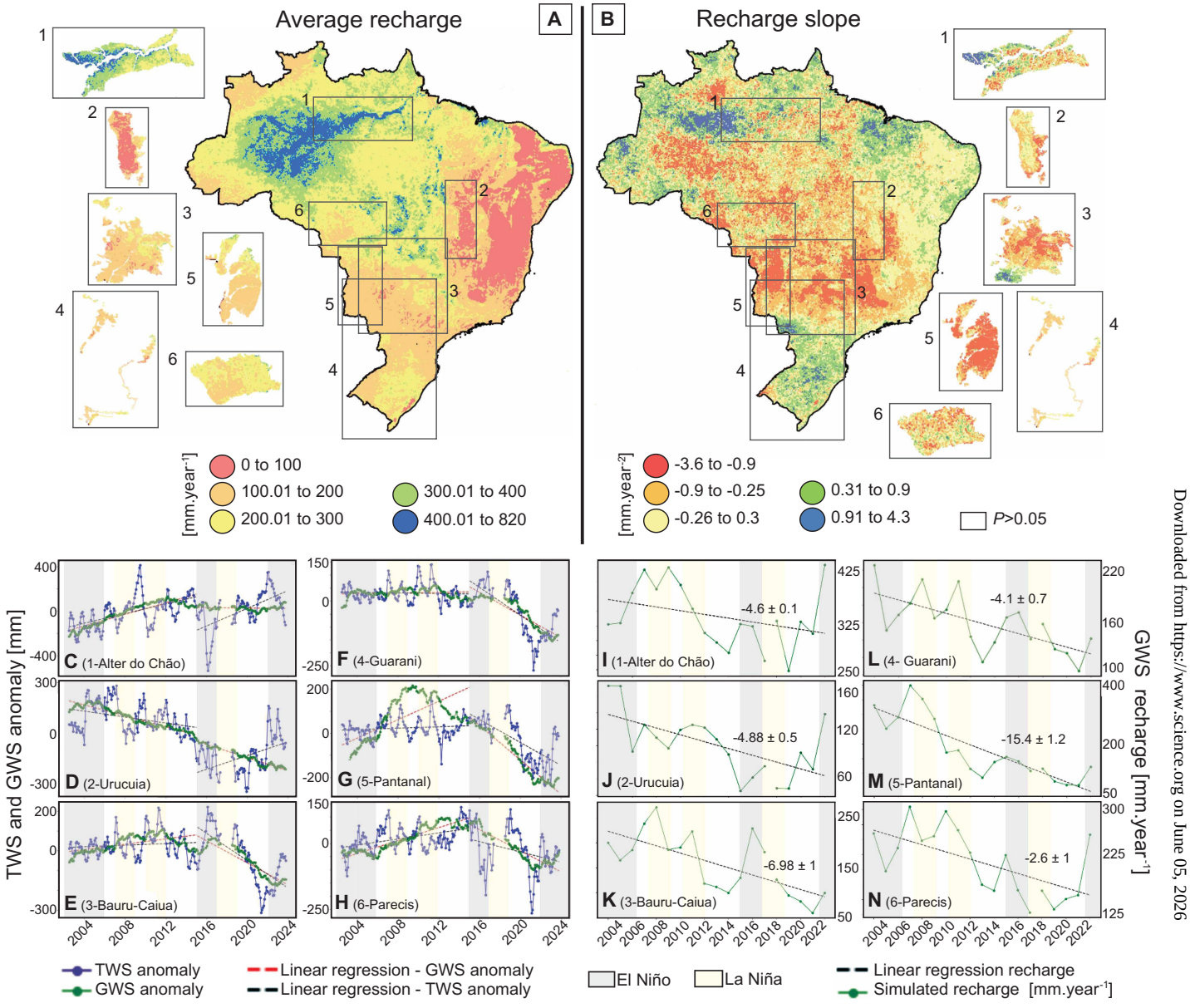

Fig. 2. Groundwater recharge dynamics and storage anomalies across major Brazilian aquifers. (**A**) Mean annual groundwater recharge (mm year^{-1}) from 2002 to 2023. (**B**) Statistically significant recharge trends (mm year^{-2}) over the same period, derived via linear regression. (**C** to **H**) Terrestrial water storage (TWS) time series, GWS anomalies for six representative aquifers in Brazil: (1) Alter do Chão, (2) Urucuia, (3) Bauru-Caiuá, (4) Guarani recharge zone (exposed portion), (5) Pantanal, and (6) Parecis. (**I** to **N**) Mean annual recharge for the same aquifers. Shaded regions indicate years corresponding to La Niña and El Niño events. Groundwater recharge estimates are based on the water table fluctuation (WTF) method. Trend values for recharge are indicated in the respective time series panels. GWS and TWS trend estimates are provided in table S1 for two time intervals: 2002–2015 and 2015–2023.

Although parts of the country were under severe drought conditions that year (*2*), the Amazon basin—covering approximately 60% of Brazil's territory—experienced anomalously high rainfall and historic flooding, which significantly contributed to the observed peak in national recharge.

It is noteworthy that certain regions in Brazil exhibit zero annual groundwater recharge, indicating an absence of replenishment during specific hydrological years. These conditions are observed in several key aquifer systems, including the Urucuia, Bauru-Caiuá, Serra Geral Formation, and the outcrop zone of the Guarani Aquifer (Botucatu Formation) (*6*, *8*, *36*). Additional zero-recharge zones include the Urucuia Aquifer, Serra Grande Formation, and areas underlain by the Crystalline Basement (Fig. 2A and fig. S2A). These patterns are primarily associated with reduced precipitation (*37*) and elevated ET rates (*38*–*40*), often exacerbated by intensive agricultural land use or water flow reaching the water table that may be in balance with groundwater runoff (*41*). Although some authors speculate that pasture insertion can increase recharge in areas, such as the Guarani or Bauru aquifers (*42*), our results suggest that land cover change may reduce GWS (fig. S3F and table S2).

Within the Paraguay River basin, a significant decline in recharge—particularly within the Pantanal aquifer (Fig. 2G and fig. S4, F and

L)—is likely driven by a combination of recent multi-year droughts (*43*, *44*) and widespread land cover changes. The region, encompassing one of the world's largest tropical wetlands, has been increasingly affected by seasonal wildfires and the encroachment of pasture lands over native vegetation (*45*).

It is important to emphasize that these estimates are subject to the influence of current groundwater extraction practices, which may suppress recharge signals, as observed in other global regions (*46*). In addition, the model captures the cumulative effects of land cover dynamics and aquifer evolution due to its regional scope and long-term design.

ENSO impacts on GWS

Figure 2 (C to N) highlights the timing of major El Niño–Southern Oscillation (ENSO) events and their relationship with anomalies in GWS and terrestrial water storage (TWS), as well as estimated recharge rates. Sensitivity analysis of the model (text S2) identified precipitation seasonality as the most influential predictor of groundwater recharge, based on SHAP (SHapley Additive exPlanations) value distributions. Sustained emerging trends in TWS are likely to reflect long-term changes in groundwater systems—particularly when hydrogeological processes, with their inherently slow response times, dominate (see fig. S6 for Mann-Kendall trend analysis of GWS across the country). For example, the consistent TWS decay observed between 2009 and 2019 (Fig. 2, E to H) is indicative of extended GWS decline.

To evaluate the hydrological impact of the 2015/2016 El Niño event on Brazil's major unconfined aquifer systems, GWS inclinations were analyzed across three periods: 2002–2023, 2002–2014 (pre-El Niño), and 2015–2023 (post-El Niño)—linear regressions for each period are shown in Fig. 2 and figs. S4 and S5, with corresponding trend values summarized in table S1. The analysis focuses on six major unconfined aquifers: Alter do Chão, Urucuia, Bauru-Caiuá, the outcrop zone of the Guarani Aquifer, Pantanal, and Parecis. Results reveal that the El Niño event exerts considerable influence on GWS variability. Strong signals of hydrological response were observed in the Amazon (Alter do Chão), Tocantins-Araguaia, Paraná (Bauru-Caiuá and Guarani), Paraguay (Pantanal), São Francisco (Urucuia), and Uruguay basins. These regions, which lie away from coastal climatic moderation, appear more sensitive to the precipitation anomalies associated with these climate oscillations. A marked shift in groundwater behavior is evident following the 2015/2016 El Niño event. The transition from weakly positive or neutral trends to widespread negative trends in GWS across several basins highlights the capacity of extreme seasonal climate events to alter long-term groundwater dynamics.

In contrast, coastal basins along the Atlantic exhibit positive trends in GWS (see figs. S4 and S5). This increase may be linked to La Niña events, which are associated with enhanced precipitation along Brazil's eastern and southeastern coastal regions (*47*–*49*). Elevated groundwater levels in these basins can reduce the sub-surface's capacity to absorb excess rainfall, thereby increasing surface runoff and the likelihood of flooding (*50*). Additionally, saturated soils can promote mass movement processes such as landslides, which have been documented during intense rainfall events in Brazil (*51*). For example, in the South Atlantic basin, GWS increased during the study period, particularly leading into 2023–2024. This rise in subsurface saturation may have limited infiltration capacity and exacerbated the severity of the flooding events that struck southern Brazil during this period (*52*, *53*). These findings are consistent with previous studies (*28*, *54*–*56*) that underscore the substantial influence of El Niño and La Niña events on hydrological processes in the Amazon and broader South American region.

Emerging trends and attributions

Spatial patterns of emerging GWS trends were identified using a support vector machine (SVM) clustering approach (*57*), resulting in seven distinct regions (Fig. 3A). Region 1 exhibited a strong positive storage trend, regions 2 and 4 showed moderate storage declines, and region 3 was characterized by severe storage depletion. No statistically significant trends were detected in regions 5 and 6. Region 7 shows a positive storage trend.

Focusing on northern Brazil, particularly the Amazon River basin (fig. S4C), a positive precipitation trend is observed (fig. S3B), which corresponds with modest gains in groundwater recharge and storage in localized areas, such as the Alter do Chão aquifer (Fig. 2, region 1, and fig. S3A). TWS variation in the region may reflect broader climate-driven processes, with some studies predicting significant impacts on GWS in the Southern Hemisphere (*58*), particularly in high-storage regions like the Amazon basin (*59*).

These findings raise an important question: Can distinct recharge and storage behaviors coexist within the same aquifer system or river basin? Comparing results presented in Figs. 2 and 3A confirms this possibility, showing that aggregate basin-scale trends may indicate net losses even when substantial subregions experience storage gains. This divergence is particularly evident in the Alter do Chão, Bauru-Caiuá, Guarani, and Parecis aquifers (Fig. 2), as well as in major basins, such as the Tocantins-Araguaia, Amazon, and Paraná (figs. S4 and S5).

In region 1, which exhibits strong positive GWS trends, increases are likely influenced by interannual climate variability, particularly El Niño and La Niña events, which modulate precipitation patterns in southern Brazil (*60*). These events contribute to elevated recharge during wetter periods, reinforcing storage gains. Region 7 exhibits positive groundwater trends—not as strong as those in region 1—mostly driven by increased precipitation rates (see fig. S3B).

In region 2, encompassing the southern Amazon River basin and much of the Tocantins-Araguaia basin, extensive conversion of tropical forest and Cerrado to agricultural land has intensified (*61*–*63*), coinciding with significant declines in observed precipitation (*37*, *38*, *63*). These combined land cover and climate shifts (see fig. S3, B and F) are linked to reduced groundwater recharge (Fig. 3B) and the resulting storage losses evident in our SVM-based regional clustering. This area also represents Brazil's new agricultural frontier, where escalating groundwater abstraction is documented (*23*, *64*–*66*). Climate projections further predict decreasing recharge rates in northern Brazil under future warming scenarios (*67*), while amplified seasonality (*7*, *68*) and large-scale deforestation (*69*, *70*) continue to alter the hydrological cycle. Thus, storage declines in region 2 arise from the synergistic impact of intensified extraction, altered hydrological processes, and land-use change, rather than abstraction alone.

Also in region 2, the decline in the Pantanal aquifer (see Fig. 2, G and M) is intensified during the 2019–2020 drought (*71*) and may reflect a shift in the recharge regime based on modeled trends. In this area, groundwater recharge is likely affected by both agricultural and hydrological droughts, often compounded by widespread fire activity (*43*, *44*). Wildfires alter soil properties, reduce infiltration

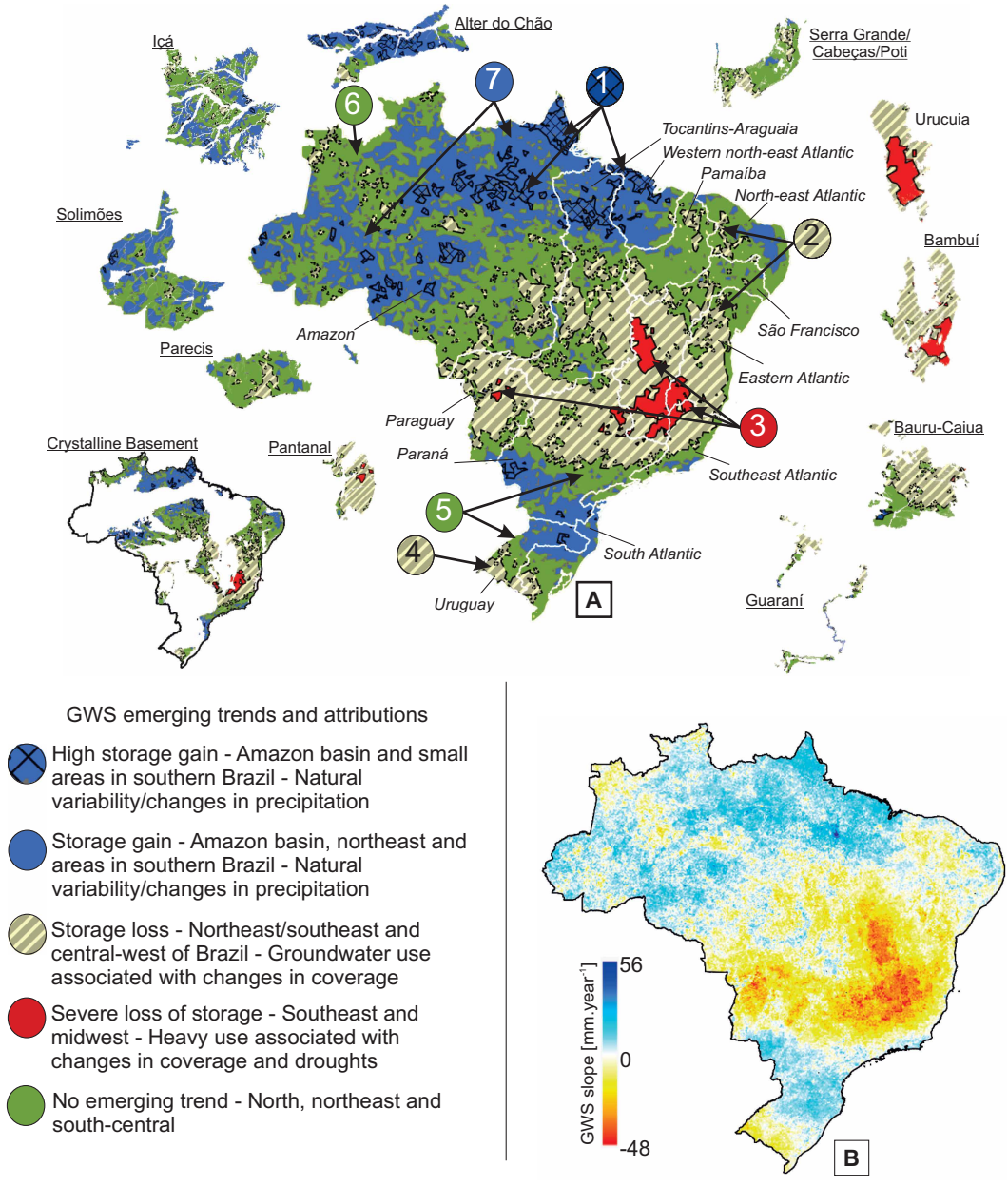

Fig. 3. Emerging GWS trends in Brazil (July 2002–October 2023). (**A**) Classification of emerging GWS trends. (**B**) GWS trend (mm year^{-1}) derived from GWS anomalies. Emerging trends in GWS were classified using a support vector machine (SVM) clustering approach (*57*) across 12 hydrographic basins—Amazon, Tocantins-Araguaia, Western Northeast Atlantic, Parnaíba, Northeast Atlantic, São Francisco, Eastern Atlantic, Southeast Atlantic, Uruguay, Paraná, South Atlantic, and Paraguay—and 11 key aquifer systems: Alter do Chão, Serra Grande-Cabeças-Poti, Urucuia, Bambuí, Bauru-Caiuá, Guarani, Pantanal, Crystalline Basement, Parecis, Solimões, and Içá. The classification captures regions of storage gain, loss, severe depletion, and neutral trends, providing spatial context for groundwater variability and stress across Brazil.

capacity, and disrupt recharge processes (*72*, *73*). Moreover, drought conditions driven or intensified by fires (*45*, *74*) may exacerbate storage losses. Given these complex interactions, this region warrants further investigation to better understand the controls on groundwater behavior and resilience under compounding environmental stressors.

In northeastern Brazil (region 2), declining GWS is primarily attributed to increased groundwater abstraction (*23*, *65*, *66*, *75*) and the occurrence of prolonged droughts (*1*, *76*, *77*). Rodell *et al.* (*78*) report a mean groundwater loss of -16.7 ± 2.9 km^3 year^{-1} in the region, with anomalously low rainfall observed in 2012, 2014, and 2015 (*1*). Climate projections suggest that recharge in this semi-arid region may decrease by up to 70% due to climate change impacts (*67*).

The most severe GWS declines are observed in central Brazil (region 3), with notable losses in the São Francisco, Paraná, Southeast Atlantic, and East Atlantic basins (figs. S4 and S5). These trends result from a compounding set of drivers, including intensive groundwater use (*23*, *65*, *75*, *79*), severe droughts (*1*, *2*, *78*), anthropogenic climate change (*28*, *37*, *58*, *80*), and shifts in the regional hydrological cycle (*7*, *68*). Collectively, these factors contribute to substantial and sustained depletion of groundwater resources across the region.

In region 4, storage losses are likely associated with localized groundwater abstraction (*5*, *65*) and natural hydrological variability. Although less pronounced than in other regions, the observed decline suggests a combination of climatic and anthropogenic influences.

DISCUSSION

Many global aquifer systems are increasingly threatened by a combination of anthropogenic pressures and environmental change, with several regions approaching critical thresholds of physical sustainability (*81*)—where groundwater withdrawal rates exceed natural and artificial recharge. In Brazil, similar pressures are emerging, particularly in large aquifers (*6*, *8*, *9*, *36*), mirroring patterns already documented in highly exploited systems such as the Central Valley (*82*) and High Plains (*83*) aquifers, in the US, the Lower Zayandeh-Rud, in Iran (*84*), and aquifers in northern India and Bangladesh (*85*), all of which exhibit severe GWS declines.

In this context, careful consideration is essential when evaluating the groundwater use potential of unconfined aquifers. Resource assessments that focus solely on extraction capacity, without incorporating regional hydrogeological behavior and the effects of climate variability, risk triggering long-term storage depletion. Such unsustainable practices have already led to persistent groundwater losses in central Brazil (*86*), underscoring the need for integrated, climate-sensitive management strategies that go beyond volumetric availability.

This study provides the first nationwide, observation-based assessment of groundwater dynamics across Brazil. We integrated local well data, socioeconomic information, and satellite-based hydrological measurements [e.g., GRACE's TWS, global precipitation measurement's (GPM) precipitation, and moderate resolution imaging spectroradiometer's (MODIS) leaf area index (LAI) and ET], and LAI (MODIS) within a machine learning framework to estimate monthly recharge over a 0.1° spatial grid between 2002 and 2023. Extensive sensitivity analyses were conducted on both model architecture and input features to ensure robustness. The final dataset encompasses nearly 20 million values for recharge estimates across 87,367 grid cells, enabling a fine-scale characterization of recharge variability and long-term changes across diverse climatic, geological, and socioeconomic settings—from individual unconfined aquifers to major river basins.

Our findings indicate that average groundwater recharge in Brazil is approximately 12% of annual precipitation, although spatial variability is considerable. Certain aquifers, particularly in northeastern and southeastern Brazil—including the Urucuia (*8*), Guarani, and Serra Geral (*87*), experience zero recharge in some years, highlighting their vulnerability to interannual climate variability. The Pantanal aquifer presents a particularly critical case, with recharge decline attributed to a combination of land-use change (*88*), precipitation anomalies, climate variability (*89*), and recurrent wildfires (*43*). These disturbances alter soil structure and reduce infiltration, compounding the effects of drought and further impairing recharge processes.

GWS estimates derived from our model are consistent with values previously reported in the literature (table S3), although training and validation were constrained by the limited availability of data from carbonate and fractured aquifers. While comparisons with estimates from indirect methods must be interpreted with caution, they nonetheless provide valuable benchmarks for large-scale validation. Overall, these results demonstrate the model's robustness and applicability across diverse hydrogeological contexts, showing strong agreement with earlier studies despite the scarcity of detailed, aquifer-scale assessments.

Our analysis reveals pronounced spatial heterogeneity in GWS variability across Brazil. The Amazon basin exhibits the largest seasonal fluctuations, a pattern linked to the region's porous sedimentary aquifers and extensive alluvial deposits, combined with high rainfall seasonality and strong river-aquifer interactions (*9*). In contrast, aquifers in central and northeastern Brazil display markedly lower seasonal variability, likely due to their lower transmissivity, limited surface water connectivity, and deeper static water levels relative to alluvial systems.

SACZ plays a pivotal role in modulating recharge dynamics, particularly during the austral summer (DJF), when enhanced moisture flux supports widespread infiltration and recharge in central and southeastern Brazil (*36*). During the dry season [March-April-May (MAM)], GWS declines are prevalent, driven by minimal recharge and elevated ET. These patterns are consistent with previous GRACE-based assessments (*1*, *77*, *78*, *90*) but offer enhanced spatial granularity, enabling the detection of localized GWS responses to seasonal and interannual climate forcing (*28*, *37*, *71*, *87*, *91*).

El Niño and La Niña events exert a significant influence on Brazil's groundwater dynamics by modulating precipitation patterns and, consequently, aquifer recharge. The 2015–2016 El Niño event resulted in pronounced GWS declines across the country (*1*), with the most substantial impacts observed in the Amazon (*92*) and Paraná basins. In contrast, La Niña episodes have been associated with enhanced recharge in coastal systems, particularly in the South Atlantic basin, due to increased precipitation (*49*).

Despite the Amazon basin's vast hydrological reserves, it experienced record-low river levels during the 2023–2024 hydrological year, coinciding with a strong El Niño and persistent long-term climate trends. Our model captures this hydroclimatic sensitivity, highlighting how both extreme droughts and floods disrupt the regional groundwater equilibrium. Similarly, the Urucuia Aquifer continues to exhibit sustained GWS losses (*6*), largely attributable to recurrent drought conditions and intensive irrigation (*93*).

Together, these findings emphasize the importance of integrating local-scale observational data into national groundwater assessments, especially in regions facing increasing hydrological stress under climate change.

Groundwater use and depletion

Groundwater depletion is a complex and increasingly global concern, with far-reaching implications for water security, land subsidence (*94*), reductions in river discharge and surface water availability discharge (*84*, *85*), salt water intrusion in coastal zones, increased pumping costs, and even potential perturbations in Earth's rotational dynamics (*95*). In Brazil, recent studies have linked groundwater losses primarily to meteorological droughts (*1*, *2*). While this study does not establish causality between groundwater depletion and extraction rates, the spatial overlap between emerging negative GWS trends and areas of high socioeconomic demand suggests a likely correlation.

Currently, groundwater serves as the sole source of water supply for approximately 40% of Brazilian municipalities (*5*) and meets a significant portion of the country's agricultural irrigation demand (*8*). The growing reliance on groundwater for irrigation has already exerted pressure on large aquifer systems (*5*).

Mining activities further exacerbate groundwater stress, particularly in regions where aquifer dewatering is required for mineral extraction (fig. S3E). Both open-pit and underground mining

operations can dramatically alter groundwater dynamics by functioning as hydraulic sinks, necessitating continuous dewatering. These processes not only deplete groundwater reserves but also disrupt natural flow regimes and may diminish surface water contributions to rivers and wetlands (*96*, *97*). The long operational life span and vertical extent of many mining projects compound these effects. For instance, in the eastern portion of the Moeda Syncline (Minas Gerais state), groundwater extraction exceeds 150% of estimated recharge—amounting to 0.04 km^3 per year over a 305 km^2 area (*98*). This imbalance results in an average annual storage decline of 134 mm, measurable even by satellite gravimetry. Such hydrological disturbances are already apparent in the São Francisco River basin and may extend into the Southeast and East Atlantic basins (see figs. S4 and S5), where groundwater–surface water interactions are increasingly altered.

To assess the multifactorial pressures on Brazil's groundwater systems, we evaluated a suite of spatial indicators, including the distribution of pivot irrigation points (*65*), well density from Brazil's Groundwater Information System (SIAGAS), areas of natural vegetation loss (*70*), mining footprints (*99*) (with emphasis on metallic mineral extraction), ET and LAI trends from NASA's MODIS, precipitation trends from NASA's GPM, and TWS trends from NASA's GRACE missions (fig. S3). This integrated analysis highlights the intersection of anthropogenic drivers and climate variability in shaping the country's evolving groundwater landscape.

Limitations

Limitations must be acknowledged. Aquifers with limited historical monitoring pose challenges due to reduced data representativeness. Additionally, regions with high variability in physical characteristics—such as geology, land use, climate, and extraction intensity—may reduce model accuracy. The model resolution (0.1°, monthly) is inherently constrained by the spatial and temporal availability of satellite data. In carbonate and crystalline terrains, although model performance is promising, further observational datasets are required to validate simulations and differentiate between regolith and bedrock contributions to storage. Moreover, although many statistical trends are attributable to human and climate forces, the 22-year study period (2002–2023) is shorter than the conventional climatological baseline of 30 years; therefore, some observed "trends" may instead reflect emerging signals influenced by interannual or decadal climate variability. Finally, as with many current AI models, the methodology is data-driven and does not explicitly incorporate physical process representations. The model's applicability to other regions or aquifers will depend on the availability and quality of input data and adherence to the method's assumptions and limitations.

Despite these constraints, the model demonstrates strong potential for capturing groundwater dynamics in diverse hydrogeological settings. The integration of satellite remote sensing and machine learning offers a scalable and transferable framework for large-scale groundwater monitoring. More broadly, this study provides new insights into the spatiotemporal behavior of Brazil's groundwater systems and represents a milestone in advancing sustainable water resources management in the country.

MATERIALS AND METHODS

The methodology developed to simulate variations in GWS in Brazil integrates satellite observations, in situ well data, and hydrogeological attributes into a data-driven AI framework. The approach comprises four main steps:

1) Time series decomposition: Satellite datasets from GRACE, MODIS, and GPM were decomposed into seasonal and wavelet components to capture dominant temporal patterns. Discrete wavelet transform components (D1, D2, D3) and seasonal (S) and trend (T) signals were extracted from each dataset.

2) Spline interpolation: The wavelet-decomposed components were resampled to their original temporal resolutions using spline interpolation, ensuring alignment with in situ data from Brazil's national groundwater monitoring network (RIMAS) (*6*).

3) Data integration and feature mapping: The interpolated satellite signals were collocated with RIMAS well data in space and time (latitude, longitude, timestamp). Hydrogeological attributes, including stratigraphic units, aquifer turnover potential, and aquifer productivity, were obtained from the Hydrogeological Map of Brazil and integrated through spatial matching with SIAGAS and Brazil's Water Agency (ANA) datasets. Additional predictors included the number of SIAGAS wells per 0.1° grid cell and average groundwater abstraction rates from the ANA Water Atlas.

4) AI-based modeling: The final step involves simulating GWS using a decision-tree ensemble model architecture. Following an extensive sensitivity analysis, the model ensemble selected included extreme gradient boosting (XGBoost) (*100*), light gradient boosting machine (LGBM) (*101*), and CatBoost (CtB) (*102*), whose outputs were subsequently refined through linear regression. Feature importance was assessed using SHAP (*103*) to quantify each input's contribution to the model's predictions. Figure 4 schematizes the AI-based modeling framework.

Model training and data structure

Groundwater level data were obtained from 398 monitoring wells of the Brazilian Geological Survey's RIMAS network, which spans major hydrogeological provinces across Brazil. The model was developed to predict GWS variation in the water column using a target dataset consisting of 34,145 observations from these wells, spanning January 2010 to October 2023 (metadata listing wells—including location and average depth—are provided in table S4). For each observation, the model received 33 input features, totaling 1,126,785 values. These inputs comprised satellite observations (MODIS ET, MODIS LAI, GPM precipitation, and GRACE TWS), their wavelet and seasonal decompositions, as well as hydrogeological and socioeconomic data from the Hydrogeological Map of Brazil, SIAGAS, and ANA databases. GRACE-derived TWS anomalies were assigned double weight (2×) due to their more comprehensive representation of terrestrial water dynamics, while all other predictors were assigned unit weight (1×). Input data were normalized, whereas the target (in situ) data were not. To remove outliers potentially associated with measurement errors or automatic sensor installation, extreme target values above the 99th and below the 1st quantiles were excluded before training. For model calibration, the dataset was initially split into 80% for training and 20% for validation, with the training subset further divided (80% for training and 20% for internal testing). Groundwater monitoring data cover the 2010–2023 period, while GRACE data span 2002–2023. Once the model was trained over 2010–2023, simulations were conducted for April 2002 through October 2023 (table S5 summarizes the training and validation procedure and datasets).

Following the reconstruction of GWS anomalies, an SVM approach (*57*) was used as a supervised classification tool to delineate

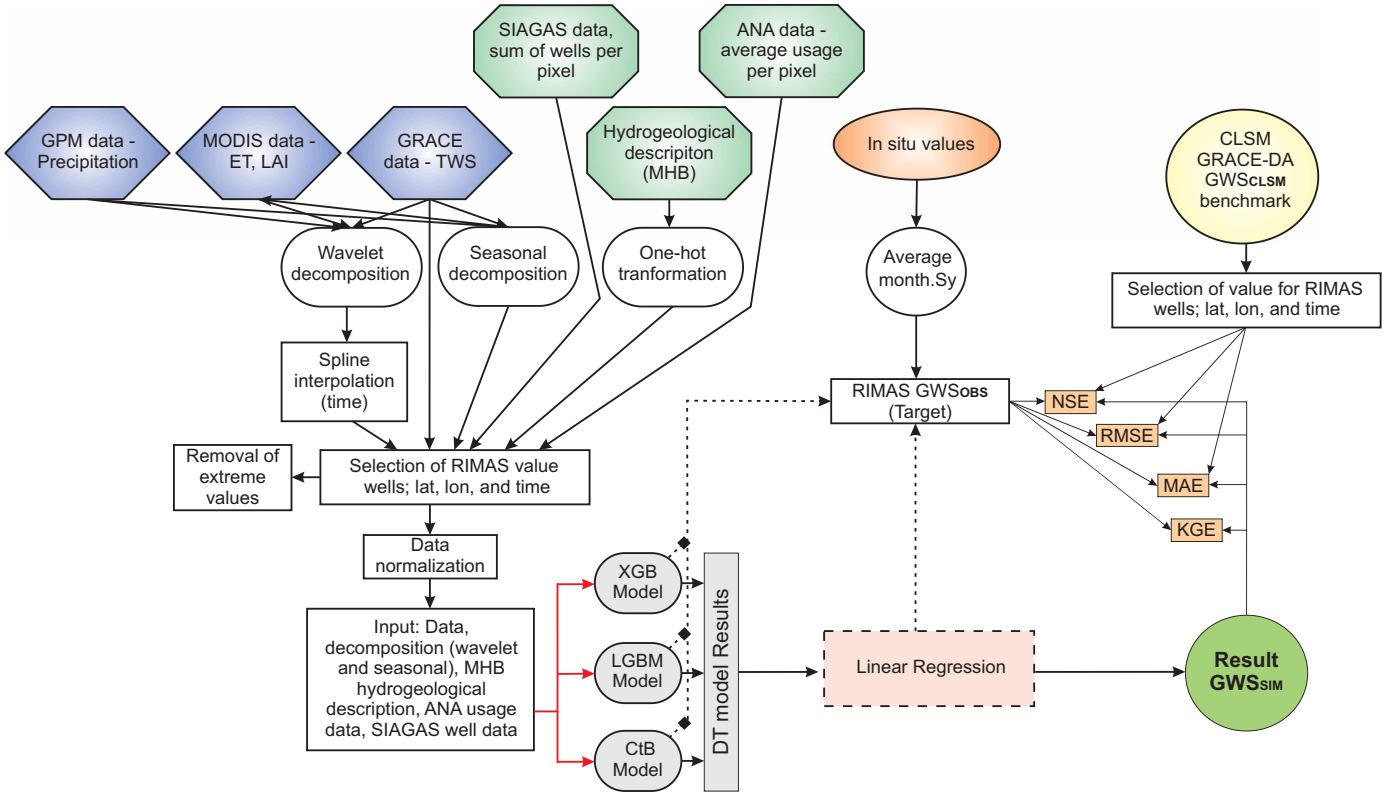

Fig. 4. Processing workflow and architecture of the AI-based joint model for groundwater simulation in Brazil. Schematic representation of the modeling framework developed to simulate GWS observations from Brazil's national monitoring network (RIMAS). The workflow integrates remote sensing inputs (MODIS ET and vegetation indices, GPM precipitation, and GRACE TWS anomalies), hydrogeological and socioeconomic datasets (SIAGAS well density and ANA water use records), and in situ well observations. Data are preprocessed via time series decomposition (seasonal and wavelet components), spatial matching, and interpolation before entering a joint AI model ensemble composed of XGBoost, LightGBM, and CatBoost algorithms. The final output simulates GWS dynamics at a national scale, validated against RIMAS observations.

hydroclimatically coherent regions. This clustering was based on a feature vector that included long-term mean precipitation, ET, and GWS trends. We utilized a radial basis function kernel, with hyperparameters (C = 1 and gamma = "scale") optimized via grid search and fivefold cross-validation. This approach ensured that the identified clusters represent physically consistent zones of groundwater behavior rather than arbitrary spatial groupings, providing a robust framework for regional-scale interpretation.

Groundwater recharge estimation

To quantify groundwater recharge across Brazil, we applied the WTF method (*32*), recognized for its effectiveness in regional-scale assessments of unconfined aquifers (*34*). The method assumes that rises in groundwater levels are predominantly due to recharge inputs reaching the water table (*35*). Recharge was computed over the period from July 2003 to October 2023 based on the GWS predicted by the model, on a simulation grid with 87,367 spatial points, throughout Brazil, with a monthly time step, resulting in nearly 20 million individual recharge simulations.

The analysis with the WTF method focused on temporal changes in groundwater level derived from the AI-based model simulations. A key advantage of this adaptation of the WTF method is that the estimated values are provided in terms of water column height, regardless of the depth or hydrogeological typology of the aquifer. This approach simplifies the analysis and extends its applicability to deep and fractured systems.

To enhance the robustness of the recharge estimates, we tested four different approaches for applying the WTF method: linear, power-law, bin mean, and bin median. The final recharge estimates were derived using the bin mean method, based on the computational framework introduced by Heppner and Nimmo (*33*). In this approach, the observed water table elevation range is divided into 20 evenly spaced elevation bins. This value was selected after sensitivity tests of 5, 10, 15, 20, 25, 50, 100, 200, and 300 intervals. During the recharge calculation, the values present in the simulation grid, excluding the year 2017, were interpolated linearly to cover the time gaps between the data, and thus apply the WTF method. Water level declines are grouped into these elevation intervals (or "compartments"), and the mean rate of decline for each bin is calculated. Recharge is then estimated by interpolating between these bin-based average decline rates to derive the recession constant for each time step. A sensitivity analysis to input data and model validation are described in texts S2 and S3.

The Monte Carlo method (*104*, *105*) was used to estimate the uncertainty of groundwater recharge by propagating random variations in the input parameters through 10,000 simulations performed for each pixel of the model grid. Two approaches were executed. First, for each run, values were sampled from a normal distribution

with a minimum SD of 0.1 mm and an initial uncertainty of 10%. The variability among the simulated results provided the final uncertainty distribution of the analyzed parameter at a 95% confidence level. The minimum SD was derived from the simulation outcomes (GWS), whereas the initial uncertainty of 10% corresponds to the model's mean absolute error (MAE). We added a second round of Monte Carlo simulations incorporating spatial variation of the specific yield (Sy) of ±10% in each pixel of the grid. Thus, different regions began to exhibit distinct Sy values relative to the model's baseline parameter (for example, reductions of ~8% in some pixels and increases of up to ~9% in others), reflecting plausible spatial heterogeneity. This new run resulted in an average uncertainty of 12.9 mm, a value lower than the uncertainty estimated in the first Monte Carlo simulation, calculated from the recharge residues. The absolute magnitude of storage and recharge is sensitive to the adopted Sy values; however, our sensitivity analysis (fig. S7) confirms that the relative spatial patterns and temporal trends remain robust. Uncertainty estimates represent lower-bound statistical uncertainty and do not account for potential structural model errors.

Limitations of the method must be recognized. For example, the WTF does not consider a constant recharge rate or allow for the unequivocal identification of the causes of WTFs. Such fluctuations do not always directly represent aquifer recharge or discharge processes, but may result from external factors, including groundwater pumping. The recharge uncertainty is directly related to that of the storage variation (ΔGWS) simulated by the model (text S3). Still, this approach provides a reasonably consistent and spatially scalable estimation of recharge, accounting for local variations in water table dynamics and allowing for application in both monitored and unmonitored regions.

Datasets

GRACE terrestrial water storage

We used Release 06 (RL06) Mascon solutions from the GRACE and GRACE-FO missions, processed by the Center for Space Research (CSR). These data span April 2002 to October 2023 at a 0.25° spatial resolution and monthly temporal resolution (*106*). GRACE provides TWS anomalies with an estimated uncertainty of approximately 1-cm water equivalent for regions ≥400,000 km^2 (*107*). Advances in GRACE processing—including the use of mascon (mass concentration) solutions—have substantially improved spatial accuracy over traditional spherical harmonic products (*108*, *109*). While the GRACE resolution remains constrained by the nature of satellite gravimetry, recent applications demonstrate the reliability of these data for hydrological assessments at sub-basin scales (*6*, *8*, *110*).

MODIS LAI and ET

LAI and ET were derived from the MODIS sensor aboard NASA's Terra and Aqua satellites (*111*). LAI estimates have been validated against in situ field measurements. Resolution varies between 250 and 500 m, depending on the specific MODIS product (*112*). ET estimates integrate surface temperature, vegetation indices, and solar radiation inputs into the Penman-Monteith equation, accounting for energy partitioning and environmental controls on transpiration, such as stomatal conductance and vapor pressure deficit (*113*).

GPM precipitation

Precipitation fields were obtained from the GPM mission via the Integrated Multi-satellite Retrievals for GPM (IMERG) algorithm (*114*). IMERG offers global coverage since 2000, with a spatial resolution of 0.1° and a 30-min temporal resolution (*115*–*117*). Despite recognized challenges in complex terrain and during calibration, GPM data have shown strong performance in Brazil, particularly when validated against ground-based observations (*118*).

In situ data: Hydrogeological map, RIMAS, SIAGAS, and ANA datasets

Hydrogeological attributes were extracted from the Hydrogeological Map of Brazil (*119*), which characterizes the spatial distribution and productivity of groundwater-bearing formations. Key model inputs included the outcropping stratigraphic unit, aquifer turnover classification, and the productivity class of each hydrostratigraphic unit.

Groundwater well attributes were sourced from SIAGAS, Brazil's Integrated Groundwater Information System (*23*), maintained by the Geological Survey of Brazil (SGB). SIAGAS includes well location, depth, and construction details. For this study, well counts were aggregated to a 0.1° grid (aligned with GPM), with zero assigned to grid cells lacking observations.

Groundwater abstraction data were derived from the Atlas Águas platform, maintained by Brazil's National Water and Sanitation Agency (ANA). We used maximum groundwater flow rates granted per municipality (in liter s^{-1}), which were then spatially interpolated and averaged over a 0.1° grid to match the spatial resolution of other input datasets.

Measurements from 398 monitoring wells within the RIMAS network provided the foundational ground-truth for assessing groundwater dynamics across approximately 2.84 million km^2 of Brazil's primary aquifer systems. These wells span porous, fractured, and karst environments, and serve as high-fidelity point constraints for the machine learning framework. Their spatial coverage is highly heterogeneous, ranging from 180 to 130,000 km^2 per well. This variability reflects the prioritization of sedimentary basins and areas of high socioeconomic importance, public water supply dependence, and natural vulnerability.

To translate the water level variation observed in the wells into the water column (the effective volume of water added to or removed from the aquifer), we multiplied the variation by the aquifer's effective porosity [see Camacho *et al.* (*6*)]. The effective porosity values applied ranged from 0.03 to 0.18, depending on the aquifer type. These water column data were crucial for optimizing the model's use of GRACE data. It is important to emphasize, however, that the large spatial variability of effective porosity in aquifers and its limited recognition are a limiting factor for both hydrogeological studies in Brazil and the results presented here.

Supplementary Materials

The PDF file includes:

Supplementary Text S1 to S3
Figs. S1 to S10
Tables S1 to S3, S5, and S6
Legend for table S4
References

Other Supplementary Material for this manuscript includes the following:

Table S4

REFERENCES

1. A. Getirana, Extreme water deficit in Brazil detected from space. *J. Hydrometeorol.* **17**, 591–599 (2016).
2. A. Getirana, R. Libonati, M. Cataldi, Brazil is in water crisis—It needs a drought plan. *Nature* **600**, 218–220 (2021).
3. A. C. Rebouças, Inserção da água subterrânea no sistema nacional de gerenciamento. *Rev. Bras. Recur. Hídricos.* **7**, 39–50 (2002).

4. FAO, *Country Profile—Brazil* (Food and Agriculture Organization, 2015).
5. Agência Nacional de Águas e Saneamento Básico, *Atlas Águas: Segurança Hídrica do Abastecimento Urbano* (Agência Nacional de Águas e Saneamento Básico, 2021).
6. C. R. Camacho, A. Getirana, O. C. Rotunno Filho, M. A. A. Mourão, Large-scale groundwater monitoring in Brazil assisted with satellite-based artificial intelligence techniques. *Water Resour. Res.* **59**, e2022WR033588 (2023).
7. V. B. P. Chagas, P. L. B. Chaffe, G. Blöschl, Climate and land management accelerate the Brazilian water cycle. *Nat. Commun.* **13**, 5136 (2022).
8. R. D. Gonçalves, R. Stollberg, H. Weiss, H. K. Chang, Using GRACE to quantify the depletion of terrestrial water storage in Northeastern Brazil: The Urucuia Aquifer System. *Sci. Total Environ.* **705**, 135845 (2020).
9. J. G. S. M. Uchôa, P. T. S. Oliveira, A. S. Ballarin, A. A. Meira Neto, D. Gastmans, S. Jasechko, Y. Fan, E. C. Wendland, Widespread potential for streamflow leakage across Brazil. *Nat. Commun.* **15**, 10211 (2024).
10. Serviço Geológico do Brasil, *Rede Integrada de Monitoramento das Águas Subterrâneas (RIMAS)* (Serviço Geológico do Brasil, 2020). https://rimasweb.sgb.gov.br/layout/.
11. B. Tapley, S. Bettadpur, M. Watkins, C. Reigber, The gravity recovery and climate experiment: Mission overview and early results. *Geophys. Res. Lett.* **31**, L09607 (2004).
12. C. E. Ndehedehe, V. G. Ferreira, O. E. Adeyeri, F. M. Correa, M. Usman, F. E. Oussou, I. Kalu, O. Okwuashi, A. O. Onojeghuo, A. Getirana, A. Dewan, Global assessment of drought characteristics in the Anthropocene. *Resour. Environ. Sustain.* **12**, 100105 (2023).
13. C. Moeck, N. Grech-Cumbo, J. Podgorski, A. Bretzler, J. J. Gurdak, M. Berg, M. Schirmer, A global-scale dataset of direct natural groundwater recharge rates: A review of variables, processes and relationships. *Sci. Total Environ.* **717**, 137042 (2020).
14. H. Tao, M. M. Hameed, H. A. Marhoon, M. Zounemat-Kermani, S. Heddam, S. Kim, S. O. Sulaiman, M. L. Tan, Z. Sa'adi, A. D. Mehr, M. F. Allawi, S. I. Abba, J. M. Zain, M. W. Falah, M. Jamei, N. D. Bokde, M. Bayatvarkeshi, M. Al-Mukhtar, S. K. Bhagat, T. Tiyasha, K. M. Khedher, N. Al-Ansari, S. Shahid, Z. M. Yaseen, Groundwater level prediction using machine learning models: A comprehensive review. *Neurocomputing* **489**, 271–308 (2022).
15. S. Razavi, B. A. Tolson, D. H. Burn, Review of surrogate modeling in water resources. *Water Resour. Res.* **48**, W07401 (2012).
16. S. Razavi, H. V. Gupta, What do we mean by sensitivity analysis? The need for comprehensive characterization of "global" sensitivity in Earth and Environmental systems models. *Water Resour. Res.* **51**, 3070–3092 (2015).
17. T. Rajaee, H. Ebrahimi, V. Nourani, A review of the artificial intelligence methods in groundwater level modeling. *J. Hydrol.* **572**, 336–351 (2019).
18. V. Nourani, N. Jabbarian Paknezhad, A. Ng, Z. Wen, D. Dabrowska, S. Üzelaltınbulat, Application of the machine learning methods for GRACE data based groundwater modeling, a systematic review. *Groundwater Sustain. Dev.* **25**, 101113 (2024).
19. C. Chen, W. He, H. Zhou, Y. Xue, M. Zhu, A comparative study among machine learning and numerical models for simulating groundwater dynamics in the Heihe River Basin, northwestern China. *Sci. Rep.* **10**, 10 (2020).
20. A. Y. Sun, B. R. Scanlon, H. Save, A. Rateb, Reconstruction of GRACE total water storage through automated machine learning. *Water Resour. Res.* **57**, e2020WR028666 (2021).
21. A. Y. Sun, Predicting groundwater level changes using GRACE data. *Water Resour. Res.* **49**, 5900–5912 (2013).
22. Y. Fan, H. Li, G. Miguez-Macho, Global patterns of groundwater table depth. *Science* **339**, 940–943 (2013).
23. Serviço Geológico do Brasil, *Sistema de Informações de Águas Subterrâneas (SIAGAS)* (Serviço Geológico do Brasil, 2020).
24. A. Getirana, C. Peters-Lidard, M. Rodell, P. D. Bates, Trade-off between cost and accuracy in large-scale surface water dynamic modeling. *Water Resour. Res.* **53**, 4942–4955 (2017).
25. G. Miguez-Macho, Y. Fan, The role of groundwater in the Amazon water cycle: 1. Influence on seasonal streamflow, flooding and wetlands. *J. Geophys. Res. Atmos.* **117**, D15113 (2012).
26. J. Bear, M. Y. Corapcioglu, Eds., *Fluid Flow in Fractured Rock: Theory and Application* (Springer Netherlands, 1991).
27. B. B. S. Singhal, R. P. Gupta, *Applied Hydrogeology of Fractured Rocks* (Springer Netherlands, 1999).
28. J. C. Espinoza, J. C. Jimenez, J. A. Marengo, J. Schongart, J. Ronchail, W. Lavado-Casimiro, J. V. M. Ribeiro, The new record of drought and warmth in the Amazon in 2023 related to regional and global climatic features. *Sci. Rep.* **14**, 8107 (2024).
29. M. A. Gan, V. E. Kousky, C. F. Ropelewski, The South America monsoon circulation and its relationship to rainfall over west-central Brazil. *J. Climate* **17**, 47–66 (2004).
30. M. S. Reboita, M. A. Gan, R. P. da Rocha, T. Ambrizzi, Regimes de precipitação na América do Sul: Uma revisão bibliográfica. *Rev. Bras. Meteorol.* **25**, 185–204 (2010).
31. B. Mueller, S. I. Seneviratne, C. Jimenez, T. Corti, M. Hirschi, G. Balsamo, P. Ciais, P. Dirmeyer, J. B. Fisher, Z. Guo, M. Jung, F. Maignan, M. F. McCabe, R. Reichle, M. Reichstein, M. Rodell, J. Sheffield, A. J. Teuling, K. Wang, E. F. Wood, Y. Zhang, Evaluation of global observations-based evapotranspiration datasets and IPCC AR4 simulations. *Geophys. Res. Lett.* **38**, L06402 (2011).
32. R. W. Healy, P. G. Cook, Using groundwater levels to estimate recharge. *Hydrgeol. J.* **10**, 91–109 (2002).
33. C. S. Heppner, J. R. Nimmo, "A computer program for predicting recharge with a master recession curve" (Scientific Investigations Report 2005-5172, U.S. Geological Survey, 2005).
34. G. Labrecque, R. Chesnaux, M.-A. Boucher, Water-table fluctuation method for assessing aquifer recharge: Application to Canadian aquifers and comparison with other methods. *Hydrgeol. J.* **28**, 521–533 (2020).
35. B. R. Scanlon, R. W. Healy, P. G. Cook, Choosing appropriate techniques for quantifying groundwater recharge. *Hydrgeol. J.* **10**, 18–39 (2002).
36. M. Donadelli Sacchi, R. Lilla Manzione, D. Gastmans, How much rainwater contributes to a spring discharge in the Guarani Aquifer System: Insights from stable isotopes and a mass balance model. *Isotopes Environ. Health Stud.* **60**, 400–416 (2024).
37. N. M. Stríkis, P. F. S. M. Buarque, F. W. Cruz, J. P. Bernal, M. Vuille, E. Tejedor, M. S. Santos, M. H. Shimizu, A. Ampuero, W. Du, G. Sampaio, H. dos Reis Sales, J. L. Campos, M. T. Kayano, J. Apaèstegui, R. R. Fu, H. Cheng, R. L. Edwards, V. C. Mayta, D. da Silva Francischini, M. A. Z. Arruda, V. F. Novello, Modern anthropogenic drought in Central Brazil unprecedented during last 700 years. *Nat. Commun.* **15**, 1728 (2024).
38. G. S. Hofmann, R. C. Silva, E. J. Weber, A. A. Barbosa, L. F. B. Oliveira, R. J. V. Alves, H. Hasenack, V. Schossler, F. E. Aquino, M. F. Cardoso, Changes in atmospheric circulation and evapotranspiration are reducing rainfall in the Brazilian Cerrado. *Sci. Rep.* **13**, 11236 (2023).
39. B. C. C. de Andrade, E. J. de Andrade Pinto, A. Ruhoff, G. B. Senay, Remote sensing-based actual evapotranspiration assessment in a data-scarce area of Brazil: A case study of the Urucuia Aquifer System. *Int. J. Appl. Earth Obs. Geoinf.* **98**, 102298 (2021).
40. A. P. M. A. Cunha, W. Buermann, J. A. Marengo, Changes in compound drought-heat events over Brazil's Pantanal wetland: An assessment using remote sensing data and multiple drought indicators. *Climate Dynam.* **62**, 739–757 (2024).
41. P. T. S. Oliveira, E. Wendland, M. A. Nearing, R. L. Scott, R. Rosolem, H. R. Da Rocha, The water balance components of undisturbed tropical woodlands in the Brazilian cerrado. *Hydrol. Earth Syst. Sci.* **19**, 2899–2910 (2015).
42. P. T. S. Oliveira, M. B. Leite, T. Mattos, M. A. Nearing, R. L. Scott, R. De Oliveira Xavier, D. M. Da Silva Matos, E. Wendland, Groundwater recharge decrease with increased vegetation density in the Brazilian cerrado. *Ecohydrology* **10**, e1759 (2017).
43. L. C. Garcia, J. K. Szabo, F. de Oliveira Roque, A. de Matos Martins Pereira, C. N. da Cunha, G. A. Damasceno-Júnior, R. G. Morato, W. M. Tomas, R. Libonati, D. B. Ribeiro, Record-breaking wildfires in the world's largest continuous tropical wetland: Integrative fire management is urgently needed for both biodiversity and humans. *J. Environ. Manage.* **293**, 112870 (2021).
44. R. Libonati, J. L. Geirinhas, P. S. Silva, D. Monteiro dos Santos, J. A. Rodrigues, A. Russo, L. F. Peres, L. Narcizo, M. E. R. Gomes, A. P. Rodrigues, C. C. DaCamara, J. M. C. Pereira, R. M. Trigo, Drought–heatwave nexus in Brazil and related impacts on health and fires: A comprehensive review. *Ann. N. Y. Acad. Sci.* **1517**, 44–62 (2022).
45. S. Kumar, A. Getirana, R. Libonati, C. Hain, S. Mahanama, N. Andela, Changes in land use enhance the sensitivity of tropical ecosystems to fire-climate extremes. *Sci. Rep.* **12**, 1–11 (2022).
46. A. Getirana, N. Kumar Biswas, S. Kumar, W. Nie, S. Ahmad, F. Maina, N. Sakib, M. S. Hossain, R. K. Biswas, Deltaic freshwater scarcity driven by unsustainable groundwater-fed irrigation. *Nat. Sustain.* **8**, 914–924 (2025).
47. V. R. Barros, A. M. Grimm, M. E. Doyle, Relationship between temperature and circulation in southeastern South America and its influence from El Nino and La Nina events. *J. Meteorol. Soc. Jpn.* **80**, 21–32 (2002).
48. A. M. Grimm, The El Niño impact on the summer monsoon in Brazil: Regional processes versus remote influences. *J. Climate* **16**, 263–280 (2003).
49. A. M. Grimm, S. E. T. Ferraz, J. Gomes, Precipitation anomalies in southern Brazil associated with El Niño and La Niña events. *J. Climate* **11**, 2863–2880 (1998).
50. N. S. Grigg, Two decades of integrated flood management: Status, barriers, and strategies. *Climate* **12**, 67 (2024).
51. V. Cabral, F. Reis, V. Veloso, C. Correa, C. Kuhn, C. Zarfl, The consequences of debris flows in Brazil: A historical analysis based on recorded events in the last 100 years. *Landslides* **20**, 511–529 (2023).
52. R. C. dos Santos Alvalá, D. F. Ribeiro, J. A. Marengo, M. E. Seluchi, D. A. Gonçalves, L. A. da Silva, L. A. C. Pineda, S. M. Saito, Analysis of the hydrological disaster occurred in the state of Rio Grande do Sul, Brazil in September 2023: Vulnerabilities and risk management capabilities. *Int. J. Disaster Risk Reduct.* **110**, 104645 (2024).
53. V. D. Pillar, G. E. Overbeck, Learning from a climate disaster: The catastrophic floods in southern Brazil. *Science* **385**, eadr8356 (2024).
54. J. L. Chen, C. R. Wilson, B. D. Tapley, The 2009 exceptional Amazon flood and interannual terrestrial water storage change observed by GRACE. *Water Resour. Res.* **46**, W12526 (2010).
55. J. A. Marengo, J. C. Espinoza, Extreme seasonal droughts and floods in Amazonia: Causes, trends and impacts. *Int. J. Climatol.* **36**, 1033–1050 (2016).

56. J. C. Espinoza, J. Ronchail, J. L. Guyot, C. Junquas, P. Vauchel, W. Lavado, G. Drapeau, R. Pombosa, Climate variability and extreme drought in the upper Solimões River (western Amazon Basin): Understanding the exceptional 2010 drought. *Geophys. Res. Lett.* **38**, L13406 (2011).
57. J. Platt, Probabilistic outputs for support vector machines and comparisons to regularized likelihood methods. *Adv. Large Margin Classif.* **10**, 61–74 (2000).
58. Y. Pokhrel, F. Felfelani, Y. Satoh, J. Boulange, P. Burek, A. Gädeke, D. Gerten, S. N. Gosling, M. Grillakis, L. Gudmundsson, N. Hanasaki, H. Kim, A. Koutroulis, J. Liu, L. Papadimitriou, J. Schewe, H. Müller Schmied, T. Stacke, C. E. Telteu, W. Thiery, T. Veldkamp, F. Zhao, Y. Wada, Global terrestrial water storage and drought severity under climate change. *Nat. Clim. Chang.* **11**, 226–233 (2021).
59. K. Hu, J. L. Awange, Khandu, E. Forootan, R. M. Goncalves, K. Fleming, Hydrogeological characterisation of groundwater over Brazil using remotely sensed and model products. *Sci. Total Environ.* **599-600**, 372–386 (2017).
60. L. G. Fernandes, R. R. Rodrigues, Changes in the patterns of extreme rainfall events in southern Brazil. *Int. J. Climatol.* **38**, 1337–1352 (2018).
61. S. Baidya Roy, R. Avissar, Impact of land use/land cover change on regional hydrometeorology in Amazonia. *J. Geophys. Res. Atmos.* **107**, 8037 (2002).
62. M. H. Costa, S. N. M. Yanagi, P. J. O. P. Souza, A. Ribeiro, E. J. P. Rocha, Climate change in Amazonia caused by soybean cropland expansion, as compared to caused by pastureland expansion. *Geophys. Res. Lett.* **34**, L07706 (2007).
63. J. A. Marengo, J. C. Jimenez, J.-C. Espinoza, A. P. Cunha, L. E. O. Aragão, Increased climate pressure on the agricultural frontier in the Eastern Amazonia–Cerrado transition zone. *Sci. Rep.* **12**, 457 (2022).
64. C. C. de A. Cajazeiras, M. A. A. Mourão, Projeto Rede Integrada de Monitoramento das Águas Subterrâneas: Relatório diagnóstico sistema aquífero Parecis no estado de Rondônia, Bacia Sedimentar dos Parecis. *Coleção Diagnóstico dos Aquíferos Sedimentares do Brasil* **8**, 40 (2012).
65. ANA, Área Irrigada—Pivôs Mapeados (2024). https://dadosabertos.ana.gov.br/datasets/41c75b31124c41ca96c14d568ba17c85_0/about.
66. R. Hirata, A. V. Suhogusoff, S. S. Marcellini, P. C. Villar, L. Marcellini, *A Revolução Silenciosa das Águas Subterrâneas no Brasil: Uma Análise da Importância do Recurso e os Riscos Pela Falta de Saneamento* (Instituto Trata Brasil, 2019).
67. R. Hirata, B. P. Conicelli, Groundwater resources in Brazil: A review of possible impacts caused by climate change. *An. Acad. Bras. Cienc.* **84**, 297–312 (2012).
68. W. Nie, S. V. Kumar, A. Getirana, L. Zhao, M. L. Wrzesien, G. Konapala, S. K. Ahmad, K. A. Locke, T. R. Holmes, B. D. Loomis, M. Rodell, Nonstationarity in the global terrestrial water cycle and its interlinkages in the Anthropocene. *Proc. Natl. Acad. Sci. U.S.A.* **121**, e2403707121 (2024).
69. C. A. Nobre, L. D. S. Borma, 'Tipping points' for the Amazon forest. *Curr. Opin. Environ. Sustain.* **1**, 28–36 (2009).
70. L. F. F. G. Assis, K. R. Ferreira, L. Vinhas, L. Maurano, C. Almeida, A. Carvalho, J. Rodrigues, A. Maciel, C. Camargo, TerraBrasilis: A spatial data analytics infrastructure for large-scale thematic mapping. *ISPRS Int. J. Geo Inf.* **8**, 513 (2019).
71. M. Calim Costa, J. A. Marengo, L. M. Alves, A. P. Cunha, Multiscale analysis of drought, heatwaves, and compound events in the Brazilian Pantanal in 2019–2021. *Theor. Appl. Climatol.* **155**, 661–677 (2024).
72. F. Vahedifard, M. Abdollahi, B. A. Leshchinsky, T. D. Stark, M. Sadegh, A. AghaKouchak, Interdependencies between wildfire-induced alterations in soil properties, near-surface processes, and geohazards. *Earth Space Sci.* **11**, e2023EA003498 (2024).
73. S. R. Maples, G. E. Fogg, R. M. Maxwell, Modeling managed aquifer recharge processes in a highly heterogeneous, semi-confined aquifer system. *Hydrgeol. J.* **27**, 2869–2888 (2019).
74. J. Tollefson, You're not imagining it: Extreme wildfires are now more common. *Nature* , (2024).
75. IBGE, *Pesquisa Nacional de Saneamento Básico* (IBGE, 2020).
76. M. Rodell, J. T. Reager, Water cycle science enabled by the GRACE and GRACE-FO satellite missions. *Nat. Water* **1**, 47–59 (2023).
77. B. Li, M. Rodell, S. Kumar, H. K. Beaudoing, A. Getirana, B. F. Zaitchik, L. G. Goncalves, C. Cossetin, S. Bhanja, A. Mukherjee, S. Tian, N. Tangdamrongsub, D. Long, J. Nanteza, J. Lee, F. Policelli, I. B. Goni, D. Daira, M. Bila, G. Lannoy, D. Mocko, S. C. Steele-Dunne, H. Save, S. Bettadpur, Global GRACE data assimilation for groundwater and drought monitoring: Advances and challenges. *Water Resour. Res.* **55**, 7564–7586 (2019).
78. M. Rodell, J. S. Famiglietti, D. N. Wiese, J. T. Reager, H. K. Beaudoing, F. W. Landerer, M.-H. Lo, Emerging trends in global freshwater availability. *Nature* **557**, 651–659 (2018).
79. R. Hirata, A. Suhogusoff, S. Susko, M. Pilar, C. Villar, L. Marcellini, *As Águas Subterrâneas e sua Importância Ambiental e Econômica para o Brasil* (IGc/USP, 2019).
80. K. Calvin, D. Dasgupta, G. Krinner, A. Mukherji, P. W. Thorne, C. Trisos, J. Romero, P. Aldunce, K. Barrett, G. Blanco, W. W. L. Cheung, S. Connors, F. Denton, A. Diongue-Niang, D. Dodman, M. Garschagen, O. Geden, B. Hayward, C. Jones, F. Jotzo, T. Krug, R. Lasco, Y.-Y. Lee, V. Masson-Delmotte, M. Meinshausen, K. Mintenbeck, A. Mokssit, F. E. L. Otto, M. Pathak, A. Pirani, E. Poloczanska, H.-O. Pörtner, A. Revi, D. C. Roberts, J. Roy, A. C. Ruane, J. Skea, P. R. Shukla, R. Slade, A. Slangen, Y. Sokona, A. A. Sörensson, M. Tignor, D. van Vuuren, Y.-M. Wei, H. Winkler, P. Zhai, Z. Zommers, J.-C. Hourcade, F. X. Johnson, S. Pachauri, N. P. Simpson, C. Singh, A. Thomas, E. Totin, A. Alegría, K. Armour, B. Bednar-Friedl, K. Blok, G. Cissé, F. Dentener, S. Eriksen, E. Fischer, G. Garner, C. Guivarch, M. Haasnoot, G. Hansen, M. Hauser, E. Hawkins, T. Hermans, R. Kopp, N. Leprince-Ringuet, J. Lewis, D. Ley, C. Ludden, L. Niamir, Z. Nicholls, S. Some, S. Szopa, B. Trewin, K.-I. van der Wijst, G. Winter, M. Witting, A. Birt, M. Ha, *IPCC, 2023: Climate Change 2023: Synthesis Report. Contribution of Working Groups I, II and III to the Sixth Assessment Report of the Intergovernmental Panel on Climate Change [Core Writing Team, H. Lee and J. Romero (eds.)]* (IPCC, 2023).
81. L. E. Condon, S. Kollet, M. F. P. Bierkens, G. E. Fogg, R. M. Maxwell, M. C. Hill, H. H. Fransen, A. Verhoef, A. F. Van Loon, M. Sulis, C. Abesser, Global groundwater modeling and monitoring: Opportunities and challenges. *Water Resour. Res.* **57**, e2020WR029500 (2021).
82. P.-W. Liu, J. S. Famiglietti, A. J. Purdy, K. H. Adams, A. L. McEvoy, J. T. Reager, R. Bindlish, D. N. Wiese, C. H. David, M. Rodell, Groundwater depletion in California's Central Valley accelerates during megadrought. *Nat. Commun.* **13**, 7825 (2022).
83. W. Nie, B. F. Zaitchik, M. Rodell, S. V. Kumar, K. R. Arsenault, B. Li, A. Getirana, Assimilating GRACE into a land surface model in the presence of an irrigation-induced groundwater trend. *Water Resour. Res.* **55**, 11274–11294 (2019).
84. S. Jasechko, H. Seybold, D. Perrone, Y. Fan, M. Shamsudduha, R. G. Taylor, O. Fallatah, J. W. Kirchner, Rapid groundwater decline and some cases of recovery in aquifers globally. *Nature* **625**, 715–721 (2024).
85. A. Getirana, N. K. Biswas, A. S. Qureshi, A. Rajib, S. Kumar, M. Rahman, R. K. Biswas, Avert Bangladesh's looming water crisis through open science and better data. *Nature* **610**, 626–629 (2022).
86. Advisory Committee on Water Information, *A National Framework for Ground-Water Monitoring in the United States* (Advisory Committee on Water Information, 2013).
87. R. Hirata, L. Goodarzi, F. S. Rörig, L. M. Alves, R. Bertolo, Climate change impacts on groundwater: A growing challenge for water resources sustainability in Brazil. *Environ. Monit. Assess.* **197**, 784 (2025).
88. J. Pompeu, Cross-boundary drivers of water cover reduction in the Pantanal wetland and implications for its conservation. *Wetlands* **45**, 32 (2025).
89. C. B. Caballero, T. W. Biggs, N. Vergopolan, L. G. G. Camelo, B. C. de Andrade, L. Laipelt, A. L. Ruhoff, Decadal hydroclimatic changes in the Pantanal, the world's largest tropical wetland. *Sci. Rep.* **15**, 17675 (2025).
90. B. Li, M. Rodell, Terrestrial water storage in 2023. *Nat. Rev. Earth Environ.* **5**, 247–249 (2024).
91. J.-C. Espinoza, J. A. Marengo, J. Schongart, J. C. Jimenez, The new historical flood of 2021 in the Amazon River compared to major floods of the 21st century: Atmospheric features in the context of the intensification of floods. *Weather Clim. Extrem.* **35**, 100406 (2022).
92. D. A. Satizábal-Alarcón, A. Suhogusoff, L. C. Ferrari, Characterization of groundwater storage changes in the Amazon River Basin based on downscaling of GRACE/GRACE-FO data with machine learning models. *Sci. Total Environ.* **912**, 168958 (2023).
93. A. F. Rodrigues, B. M. Brentan, M. V. Ottoni, J. S. Amorim, M. A. A. Mourão, N. Curi, J. C. Avanzi, C. R. de Mello, Has unsustainable groundwater use induced low flow regimes in the Urucuia Aquifer System? An urgent call for integrated water management. *J. Environ. Manage.* **370**, 122979 (2024).
94. L. F. Konikow, E. Kendy, Groundwater depletion: A global problem. *Hydrgeol. J.* **13**, 317–320 (2005).
95. K. Seo, D. Ryu, J. Eom, T. Jeon, J. Kim, K. Youm, J. Chen, C. R. Wilson, Drift of Earth's pole confirms groundwater depletion as a significant contributor to global sea level rise 1993–2010. *Geophys. Res. Lett.* **50**, e2023GL103509 (2023).
96. G. Prokop, P. L. Younger, K. E. Roehl, *Groundwater Management in Mining Areas* [Federal Environment Agency (Austria), 2004].
97. B. Lottermoser, "Mine water" in *Mine Wastes* (Springer Berlin Heidelberg, 2003), vol. 32, pp. 83–141.
98. C. C. de Castro Magalhães, M. C. de Melo, N. Guiguer, R. S. de Paula, The Cauê Aquifer on the eastern limb of the Moeda Syncline: Characterization, impacts, and flow in the western Iron Quadrangle (Quadrilátero Ferrífero), MG, Brazil. *Braz. J. Geol.* **52**, e20210086 (2022).
99. Agência Nacional de Mineração, *Processos Minerários Ativos—Brasil* (Agência Nacional de Mineração, 2024).
100. T. Chen, C. Guestrin, "XGBoost" in *Proceedings of the 22nd ACM SIGKDD International Conference on Knowledge Discovery and Data Mining* (ACM, 2016), vols. 13–17, pp. 785–794.
101. G. Ke, Q. Meng, T. Finley, T. Wang, W. Chen, W. Ma, Q. Ye, T. Y. Liu, LightGBM: A highly efficient gradient boosting decision tree. *Adv. Neural Inf. Process. Syst.* **30**, 3147–3155 (2017).
102. L. Prokhorenkova, G. Gusev, A. Vorobev, A. V. Dorogush, A. Gulin, CatBoost: Unbiased boosting with categorical features. *Adv. Neural Inf. Process. Syst.* **31**, 6638–6648 (2017).

103. S. Lundberg, S.-I. Lee, A unified approach to interpreting model predictions. *Adv. Neural Inf. Process. Syst.* **30**, 4766–4775 (2017).
104. N. Metropolis, S. Ulam, The Monte Carlo method. *J. Am. Stat. Assoc.* **44**, 335–341 (1949).
105. K. Beven, A. Binley, The future of distributed models: Model calibration and uncertainty prediction. *Hydrol. Process.* **6**, 279–298 (1992).
106. H. Save, S. Bettadpur, B. D. Tapley, High-resolution CSR GRACE RL05 mascons. *J. Geophys. Res. Solid Earth* **121**, 7547–7569 (2016).
107. S. Swenson, J. Wahr, P. C. D. Milly, Estimated accuracies of regional water storage variations inferred from the Gravity Recovery and Climate Experiment (GRACE). *Water Resour. Res.* **39**, 1223 (2003).
108. D. D. Rowlands, S. B. Luthcke, J. J. McCarthy, S. M. Klosko, D. S. Chinn, F. G. Lemoine, J.-P. Boy, T. J. Sabaka, Global mass flux solutions from GRACE: A comparison of parameter estimation strategies—Mass concentrations versus Stokes coefficients. *J. Geophys. Res.* **115**, B01403 (2010).
109. P. Ditmar, Conversion of time-varying Stokes coefficients into mass anomalies at the Earth's surface considering the Earth's oblateness. *J. Geod.* **92**, 1401–1412 (2018).
110. M. D. Melati, A. S. Fleischmann, F. M. Fan, R. C. D. Paiva, G. B. Athayde, Estimates of groundwater depletion under extreme drought in the Brazilian semi-arid region using GRACE satellite data: Application for a small-scale aquifer. *Hydrgeol. J.* **27**, 2789–2802 (2019).
111. NASA Earth Science Data Systems, MODIS/Terra Net Evapotranspiration 8-Day L4 Global 500m SIN Grid V061 | NASA Earthdata, Earth Science Data Systems, NASA (2025); https://www.earthdata.nasa.gov/data/catalog/lpcloud-mod16a2-061.
112. R. Myneni, Y. Knyazikhin, T. Park, MODIS Collection 6 (C6) LAI/FPAR product user's guide. NASA EOSDIS Land Processes DAAC (2020); https://doi.org/10.5067/MODIS/MOD15A2H.061.
113. Q. Mu, F. A. Heinsch, M. Zhao, S. W. Running, Development of a global evapotranspiration algorithm based on MODIS and global meteorology data. *Remote Sens. Environ.* **111**, 519–536 (2007).
114. G. Huffman, D. Bolvin, D. Braithwaite, K. Hsu, R. Joyce, *NASA Global Precipitation Measurement (GPM) Integrated Multi-satellitE Retrievals for GPM (IMERG)—Algorithm Theoretical Basis Document (ATBD)* (NASA, 2018).
115. A. S. Falck, V. Maggioni, J. Tomasella, D. A. Vila, F. L. R. Diniz, Propagation of satellite precipitation uncertainties through a distributed hydrologic model: A case study in the Tocantins-Araguaia basin in Brazil. *J. Hydrol.* **527**, 943–957 (2015).
116. R. Zubieta, A. Getirana, J. C. Espinoza, W. Lavado-Casimiro, L. Aragon, Hydrological modeling of the Peruvian–Ecuadorian Amazon Basin using GPM-IMERG satellite-based precipitation dataset. *Hydrol. Earth Syst. Sci.* **21**, 3543–3555 (2017).
117. A. Getirana, D. Kirschbaum, F. Mandarino, M. Ottoni, S. Khan, K. Arsenault, Potential of GPM IMERG precipitation estimates to monitor natural disaster triggers in urban areas: The case of Rio de Janeiro, Brazil. *Remote Sens.* **12**, 4095 (2020).
118. A. N. Gadelha, V. H. R. Coelho, A. C. Xavier, L. R. Barbosa, D. C. D. Melo, Y. Xuan, G. J. Huffman, W. A. Petersen, C. das N. Almeida, Grid box-level evaluation of IMERG over Brazil at various space and time scales. *Atmos. Res.* **218**, 231–244 (2019).
119. J. A. O. Diniz, L. F. C. Bomfim, M. A. de Freitas, A. B. Monteiro, A. de C. Cardoso, A. S. Franzini, C. J. B. de Aguiar, D. R. A. da Silva, G. N. dos Santos, H. R. da Silva, J. A. O. Diniz, J. L. F. Machado, L. A. Martins, L. A. da C. Pereira, M. J. da T. G. Galvão, M. M. (in Memoriam), O. A. de S. Filho, P. P. Araújo, R. R. S. Roberto, E. Kirchhein, T. L. F. de Paula, *Mapa Hidrogeológico do Brasil* (Serviço Geológico do Brasil, 2014).
120. R. D. Gonçalves, E. H. Teramoto, H. K. Chang, Regional groundwater modeling of the Guarani Aquifer System. *Water* **12**, 2323 (2020).
121. P. Galvão, R. Hirata, B. Conicelli, Estimating groundwater recharge using GIS-based distributed water balance model in an environmental protection area in the city of Sete Lagoas (MG) , Brazil. *Environ. Earth Sci.* **77**, 1–16 (2018).
122. "Groundwater management in Brazil: Current status and challenges for sustainable utilization" in *Global Groundwater* (Elsevier, 2021), pp. 409–423.
123. P. Girard, C. J. Da Silva, M. Abdo, River–groundwater interactions in the Brazilian Pantanal. The case of the Cuiabá River. *J. Hydrol.* **283**, 57–66 (2003).
124. C. R. Camacho, A. Getirana, M. A. A. Mourão, O. C. Rotunno Filho, *Avaliação da Capacidade de Modelos de Aprendizado de Máquina Quanto ao Reconhecimento ra Variação das Águas Subterrâneas no Aquífero Parecis—Brasil* (ABRHidro, 2021), pp. 1–10.
125. P. Galvao, J. G. A. Demétrio, E. L. D. Souza, M. M. Baessa, M. M. Baessa, Modelagem Numérica do Sistema Aquífero Içá-Solimões para Fins de Disponibilidade e Demanda Hídrica da Província Petrolífera de Urucu, Amazonas, Brasil. *Águas Subter.* **37**, e30282 (2023).
126. F. Correia Filho, J. Andrade, A. Monteiro, S. Fontes, E. Feitosa, A. Soares Fillho, N. Sousa, M. Barradas, Aquífero serra grande: Hidrogeologia e modelo tectônico - borda sudeste da bacia sedimentar do parnaíba - pi. *Águas Subter.* **0**, 1–20 (2010).
127. L. S. Shapley, "A value for n-person games" in *Contributions to the Theory of Games (AM-28), Volume II* (Princeton Univ. Press, 1953), pp. 307–318.
128. M. A. Moghaddam, "Application and limitation of deep learning algorithms to hydrogeology—Data driven approaches to understanding effective hydraulic conductivity, flux, and monitoring network design," thesis, University of Arizona, Tucson, AZ (2020).
129. D. Yamazaki, D. Ikeshima, J. Sosa, P. D. Bates, G. H. Allen, T. M. Pavelsky, MERIT Hydro: A high-resolution global hydrography map based on latest topography dataset. *Water Resour. Res.* **55**, 5053–5073 (2019).
130. Agência Nacional de Água, *Avaliação dos Aquíferos das Bacias Sedimentares da Província Hidrogeológica Amazonas no Brasil (escala 1:1.000.000) e Cidades Pilotos (escala 1:50.000) (Volume III—Hidrogeologia e Modelo Numérico de Fluxo da PHA no Brasil)* (Agência Nacional de Água, 2015).
131. L. V. Santarosa, D. Gastmans, T. P. Sitolini, R. E. Kirchheim, S. B. Betancur, M. E. D. De Oliveira, J. C. V. Campos, R. L. Manzione, Assessment of groundwater recharge along the Guarani aquifer system outcrop zone in São Paulo State (Brazil): An important tool towards integrated management. *Environ. Earth Sci.* **80**, 95 (2021).
132. A. da C. Reboucas, "Recursos hídricos subterrâneos da Bacia do Paraná: Análise de pré-viabilidade," thesis, USP, São Paulo, Brazil (1976).
133. UNESCO, Síntese Hidrogeológica do Sistema Aquífero Guarani (Hidrogeología local del area piloto Ribeirão Preto-IV); https://www.ceregas.org/publicaciones/proteccion-ambiental-y-desarrollo-sostenible-del-sistema-acuifero-guarani-sag/.
134. A. A. Gómez, L. B. Rodríguez, L. S. Vives, The Guarani Aquifer System: Estimation of recharge along the Uruguay–Brazil border. *Hydrgeol. J.* **18**, 1667–1684 (2010).
135. COGERH, *Relatório Final do Balanço Hídrico Considerando a Demanda e Oferta por Município* (COGERH, 2017).
136. M. Alvares Tenenwurcel, M. Soares De Moura, A. Monteiro Da Costa, P. Karen Mota, J. H. Moreira Viana, L. F. S. Fernandes, F. A. Leal Pacheco, An improved model for the evaluation of groundwater recharge based on the concept of conservative use potential: A study in the river Pandeiros Watershed, Minas Gerais, Brazil. *Water* **12**, 1001 (2020).
137. M. E. Ribeiro, T. A. Bortolin, P. A. R. Reginato, Relationship between precipitation events and groundwater recharge of the Serra Geral Aquifer System in an experimental watershed located in the municipality of Caxias do Sul, RS: Brazil. *Environ. Earth Sci.* **82**, 314 (2023).
138. V. M. Borges, F. M. Fan, P. A. R. Reginato, G. B. Athayde, Groundwater recharge estimating in the Serra Geral aquifer system outcrop area—Paraná State, Brazil. *Águas Subter.* **31**, 338 (2017).
139. L. T. P. Braga, L. N. M. Velásquez, P. M. Fleming, Groundwater recharge through the dolines in the semi-arid climate in Minas Gerais State, Brazil. *Environ. Earth Sci.* **79**, 36 (2020).
140. A. J. Cambraia Neto, L. N. Rodrigues, Evaluation of groundwater recharge estimation methods in a watershed in the Brazilian Savannah. *Environ. Earth Sci.* **79**, 140 (2020).
141. C. S. Schuch, P. Galvão, M. C. De Melo, S. Pereira, Overexploitation assessment in an urban karst aquifer: The case of Sete Lagoas (MG) , Brazil. *Environ. Res.* **236**, 116820 (2023).
142. I. Carranco, R. Hirrata, C. Marques, B. Conicelli, L. Goodarzi, F. Rörig, V. F. Boico, S. Procel, I. Hirata, Improving recharge estimates in the Bauru Aquifer System: A spatiotemporal approach using WTF. SSRN [Preprint] (2025). https://doi.org/10.2139/ssrn.5437868.
143. G. Z. S. Eger, G. C. Silva Junior, E. A. G. Marques, B. R. C. Leão, D. G. T. B. Da Rocha, T. E. Gilmore, L. G. H. Do Amaral, J. A. O. Silva, C. Neale, Recharge assessment in the context of expanding agricultural activity: Urucuia Aquifer System, western State of Bahia, Brazil. *J. South Am. Earth Sci.* **112**, 103601 (2021).
144. E. A. G. Marques, G. C. Silva Junior, G. Z. S. Eger, A. M. Ilambwetsi, P. Raphael, T. N. Generoso, J. Oliveira, J. N. Júnior, Analysis of groundwater and river stage fluctuations and their relationship with water use and climate variation effects on Alto Grande watershed, Northeastern Brazil. *J. South Am. Earth Sci.* **103**, 102723 (2020).
145. M. C. Abreu, M. G. Rocha, T. E. Vasconcelos, F. de Souza, N. de L. Oliveira, A. Gustavo, "Estimativa da recarga nos poços de monitoramento do projeto RIMAS no sistema aquífero Parecis pelo método de variação do nível d'água (VNA)" in *ABRHidro* (ABRHidro, 2017), vol. 1, p. 8.

Acknowledgments

Funding: This work was funded by the Geological Survey of Brazil, Brazilian Coordination for the Improvement of Higher Education Personnel (CAPES), the Brazilian Council for Scientific and Technological Development (CNPq), and the Rio de Janeiro State Foundation for Research Support (FAPERJ). **Author contributions:** A.G.: Writing—original draft, conceptualization, investigation, writing—review and editing, methodology, validation, supervision, formal analysis, project administration, and visualization. C.R.C.: Writing—original draft, conceptualization, investigation, writing—review and editing, methodology, resources, funding acquisition, data curation, validation, supervision, formal analysis, software, project administration, and visualization. M.A.A.M.: Conceptualization, investigation, writing—review and editing, methodology, and validation. O.C.R.F.: Conceptualization, writing—review and editing, methodology, resources, funding acquisition, validation, supervision, and project administration. **Competing interests:** The authors declare that they have no competing interests. **Data, code, and materials availability:** All software, compiled data, and instructions needed to replicate the results obtained in this study are available through

https://doi.org/10.6084/m9.figshare.29594093. This study benefitted from data derived from the following satellite missions: MODIS (https://doi.org/10.5067/modis/mcd15a3h.061, https://doi.org/10.5067/modis/mod16a2.006), GRACE (https://www2.csr.utexas.edu/grace/RL0603_mascons.html), GPM, https://disc.gsfc.nasa.gov/datasets/GPM_3IMERGM_07/summary), as well as data from RIMAS (https://rimasweb.sgb.gov.br/layout/), SIAGAS (https://siagasweb.sgb.gov.br/layout/), hydrogeological map of Brazil (https://rigeo.sgb.gov.br/handle/doc/15556), and ANA (http://atlas.ana.gov.br). Geological and hydrogeological profiles for all monitored aquifers are available at https://www.sgb.gov.br/colecao-de-relatorios-diagnostico-dos-aquiferos-sedimentares-do-brasil. This study did not generate new materials.

Submitted 18 November 2025
Accepted 21 April 2026
Published 3 June 2026
10.1126/sciadv.aee0266

ScienceAdvances

Two decades of human- and climate-induced groundwater storage shifts in Brazil

Augusto Getirana, Clyvihk Renna Camacho, Maria Antonieta A. Mourão, and Otto Corrêa Rotunno Filho

Sci. Adv. **12** (23), eaee0266. DOI: 10.1126/sciadv.aee0266